PA-X is a virulence factor in avian H9N2 influenza virus

Huijie Gao [1,†], Guanlong Xu [1,†], Yipeng Sun [1,†], Lu Qi [1], Jinliang Wang [1], Weili Kong [1], Honglei Sun [1], Juan Pu [1], Kin-Chow Chang [2], and Jinhua Liu [1,#]

[1] Key Laboratory of Animal Epidemiology and Zoonosis, Ministry of Agriculture, College of Veterinary Medicine and State Key Laboratory of Agrobiotechnology, China Agricultural University, Beijing, China

[2] School of Veterinary Medicine and Science, University of Nottingham, Sutton Bonington Campus, United Kingdom

[#]Corresponding author. Key Laboratory of Animal Epidemiology and Zoonosis of the Ministry of Agriculture, College of Veterinary Medicine and State Key Laboratory of Agrobiotechnology, China Agricultural University, No. 2 Yuanmingyuan West Road, Beijing 100193, China.

Tel: +86-10-62733837; Fax: +86-10-62733837; E-mail: ljh@cau.edu.cn

[†] Huijie Gao, Guanlong Xu and Yipeng Sun contributed equally to this work.

Running title: Contribution of PA-X to the virulence of the H9N2 virus

Content Category: Animal Viruses - Negative-strand RNA

Word counts: Summary: 194; Main text: 3716.

Tables and figures: 5.

Summary

H9N2 influenza viruses have been circulating worldwide in multiple avian species and regularly infect pigs and humans. Recently, a novel protein PA-X, produced from the PA gene by ribosomal frameshifting, is demonstrated to be an anti-virulence factor in pandemic 2009 H1N1, highly pathogenic avian H5N1 and 1918 H1N1 viruses. However, a similar role of PA-X in the prevalent H9N2 avian influenza viruses has not been established. In this study, we compared the virulence and cytopathogenicity H9N2 wild type virus and H9N2 PA-X deficient virus. Loss of PA-X in H9N2 virus reduced apoptosis and had marginal effect on progeny virus output in human pulmonary adenocarcinoma (A549) cells. Without PA-X, PA was less able to suppress co-expressed green fluorescence protein (GFP) in human 293T cells. Furthermore, absence of PA-X in H9N2 virus attenuated viral pathogenicity in mice which showed no mortality, reduced progeny virus production, mild to normal lung histopathology, and dampened proinflammatory cytokine and chemokine response. Therefore, unlike previously reported H1N1 and H5N1 viruses, we show that PA-X protein in H9N2 virus is a pro-virulence factor in facilitating viral pathogenicity, and that the pro- or anti-virulence role of PA-X in influenza viruses is virus-strain dependent.

Keywords: H9N2 influenza virus; PA-X; Pathogenicity

Introduction

H9N2 influenza viruses have been circulating worldwide in poultry resulting in severe economic losses due to reduced egg production or increased mortality associated with co-infection with secondary pathogens (Banks *et al.*, 2000; Bano *et al.*, 2003; Capua & Alexander, 2006). H9N2 influenza viruses have been widely reported to infect mammals, including pigs and humans (Abolnik *et al.*, 2010; Butt *et al.*, 2010; Cong *et al.*, 2007; Sun *et al.*, 2010; Xu *et al.*, 2007); there is evidence that a large number of people have been infected with H9N2 viruses in particular poultry workers (Coman *et al.*, 2013; Jia *et al.*, 2009; Wang *et al.*, 2009). H9N2 virus infections in humans showed typical human flu-like symptoms which can easily go undetected or unreported (Butt et al., 2005; Lin et al., 2000). Recent studies showed that H9N2 viruses contributed the six internal genes to the novel H7N9 and H10N8 viruses that are causing severe human infections in China (Chen et al., 2014; Gao et al., 2013; Zhang et al., 2013). H9N2 viruses can be regarded as precursors to emerging subtypes of influenza viruses that are highly infectious to humans. Therefore, it is important to ascertain virulence factors of H9N2 viruses.

Recently, PA-X, arising from ribosomal frame-shift in a +1 open reading frame (X-ORF) extension of a growing PA polypeptide, was identified as a protein (Jagger et al., 2012). It was demonstrated that PA-X plays an important role in inhibiting cellular protein synthesis, suggesting that PA-X contributes to host-cell shut off induced by influenza virus (Desmet et al., 2013; Jagger et al., 2012; Katze et al., 1986a; Katze et al., 1986b). Jagger *et al.* also showed that PA-X decreased the

virulence of the 1918 H1N1 virus in a mouse model, through modulating host inflammatory response, apoptosis, cell differentiation and tissue remodeling (Jagger et al., 2012). We recently reported that loss of PA-X expression in 2009 pandemic H1N1 (pH1N1) and highly pathogenic H5N1 viruses increases viral replication and apoptosis in A549 cells and increases virulence and host inflammatory response in mice (Gao et al., 2015). Loss of PA-X expression also increases the virulence and virus replication of H5N1 virus in avian species, and blunts the host innate immune and cell death response (Hu et al., 2015).

Here we report that the absence of PA-X in H9N2 virus, contrary to previous findings on pH1N1, highly pathogenic H5N1 and 1918 H1N1 viruses, decreases viral replication and pro-inflammatory response in mice. The absence of PA-X in H9N2 virus also reduces virus-induced suppression of cellular protein synthesis.

Results

Generation of PA-X deficient H9N2 virus

In the present study, the use of reverse genetics was based on the A/chicken/Hebei/LC/2008 (H9N2 WT) virus (Sun et al., 2011). To evaluate the effect of loss of PA-X expression on viral function, we generated PA-X deficient virus, H9N2-FS, by altering the frameshifting motif from UCC UUU CGU to AGC UUC AGA in the PA segment to prevent the formation of PA-X (Fig.1a) (Jagger et al., 2012). The mutations did not alter the PA ORF. To show that PA-X expression from H9N2-FS was abolished, Madin Darby Canine Kidney (MDCK) cells were infected

with H9N2 PA-X mutant and WT viruses at an MOI of 1, and cell lysates were harvested at 12 hpi. We found that PA-X could be detected in H9N2 WT infected cells but not in H9N2-FS infected cells (Fig.1b).

Decreased apoptosis in A549 cells infected with PA-X deficient H9N2 virus

H9N2 WT and H9N2-FS were used to infect MDCK and human pulmonary adenocarcinoma (A549) cells at an MOI of 0.01, and the supernatants were collected and titrated at 6, 12, 24, 36, 48, 60, 72 and 84 h post infection (hpi). There was no significant difference in the virus output from MDCK cells between H9N2 WT and H9N2-FS viruses (Fig.2a). In A549 cells, H9N2-FS and H9N2WT viruses reached maximum virus output at around the same time (48 hpi) with comparable peak virus titers; viral titers at indicated time points showed no significant difference between H9N2-FS and H9N2 WT virus (Fig.2b).

Apoptosis is a contributor to virulence (Roberts & Nichols, 1989; Tumpey *et al.*, 2000). Some viral proteins are able to induce apoptosis, such as NS1 and PB1-F2 (Chanturiya *et al.*, 2004; Chen *et al.*, 2001; Zhirnov *et al.*, 2002). A549 cells were infected with H9N2-FS and WT viruses at an MOI of 1 for 6 and 12 h and assessed for apoptosis. H9N2-FS virus infection produced less apoptotic cells (1.40% annexin V+ only at 6 hpi and 6.59% at 12 hpi) than H9N2 WT virus (3.60% at 6 hpi and 10.73% at 12hpi) ($P < 0.05$) (Fig.2c). Cells that were PI+ only, and annexin V+ PI+ showed no significant difference between H9N2-FS and H9N2 WT viruses. Overall, the data show that loss of PA-X in H9N2 virus has little effect on viral replication and produced less apoptosis in A549 cells.

PA-X deficient H9N2 virus is less pathogenic and causes mild inflammatory response in mice relative to H9N2 wild type virus

To assess the effect of PA-X on pathogenicity, mice (15 per group) were intranasally inoculated at 10^6 $TCID_{50}$ with each virus. Clinical signs, mortality and weight loss were monitored over 14 days. Three virus-infected mice a day were humanely killed at 3, 5, and 7 days post infection (dpi), and lungs were collected for virus titration. H9N2-FS virus infection resulted in no death, while H9N2 WT infection caused 33.3% mortality (Fig. 3a). No significant weight loss was observed in the H9N2-FS virus infected group, in contrast to the 15% weight loss of H9N2 WT virus infected mice (Fig. 3b).

Histopathologically, H9N2-FS virus infected lung appeared nearly normal. However, in the H9N2 WT virus group, there were extensive vascular congestion, and cellular exudate (Fig. 3c). Viral titers of H9N2-FS virus infected lungs were 8-20 fold lower than those of H9N2 WT virus at 3, 5 and 7 dpi ($P < 0.05$) (Fig. 3d) consistent with the observed pathology.

Increased pulmonary cytokine/chemokine expression contributes to the severity of influenza virus infection in humans and animal models (Bermejo-Martin et al., 2010; Hagau et al., 2010; Lam et al., 2010; Perrone et al., 2008). We determined the protein levels of seven cytokines and chemokines in the lungs of H9N2 WT and H9N2-FS virus infected mice at 3 and 5 dpi. Interleukin-1β (IL-1β), interleukin-6 (IL-6), the mouse equivalent of human IL-8 (KC), monocyte chemotactic protein 1 (MCP-1), macrophage inflammatory protein-1α (MIP-1α or CCL3), tumor necrosis factor-alpha

(TNF-α) and interferon gamma (IFN-γ) levels from H9N2-FS virus infected mice were consistently lower than those of H9N2 WT virus infected mice at both time points ($P < 0.05$) (Fig.4). Collectively, these results demonstrate that PA-X in H9N2 virus facilitates pathogenicity and up-regulated inflammatory response in mice.

PA protein is less effective at suppressing protein expression without PA-X

Inhibition of host protein synthesis by influenza virus can hinder host anti-viral response and promote virus replication (Katze *et al.*, 1986a; Katze *et al.*, 1986b). PA gene plays a major role in the suppression of host protein synthesis, which is partly mediated by PA-X (Desmet et al., 2013; Jagger et al., 2012). We compared the ability of PA of H9N2 WT and H9N2-FS viruses to suppress non-viral protein synthesis by co-transfections of Human embryonic kidney (293T) cells for 24 h with H9N2 WT PA or H9N2-FS PA, and pEGFP expression plasmids. eGFP expression was significantly higher by more than 20% when co-transfected with H9N2-FS PA, compared with H9N2 WT PA co-transfection (Fig.5a & b). Although the expression level of PA protein of H9N2-FS was higher than that of H9N2 WT, H9N2-FS PA plasmid was less effective in suppressing eGFP expression than H9N2 WT PA (Fig.5b). These results suggest that loss of PA-X in H9N2 virus reduces the host shut off ability of the virus in 293T cells.

Discussion

In the present study, we assessed the pathogenic capability of PA-X in avian H9N2 virus. PA-X deficient H9N2 (H9N2-FS) virus was less virulent than its H9N2

157 WT counterpart. Absence of PA-X attenuated the H9N2 virus manifested as decreased
158 viral replication, reduced apoptosis and dampened pro-inflammatory response.
159 Furthermore, PA without PA-X was less able to suppress host protein synthesis.
160 Therefore, we propose that PA-X in H9N2 virus is a virulence factor.

161 Previous studies, however, have shown that PA-X deficient-H1N1 and -H5N1
162 viruses are more pathogenic than their corresponding WT counterparts (Gao et al.,
163 2015; Hu et al., 2015; Jagger et al., 2012). Enhanced virulence of the 1918 H1N1
164 virus deficient in PA-X might be due to alterations in the kinetics of host response
165 (Jagger et al., 2012). Jagger *et al.* (2012) found that loss of PA-X expression in the
166 1918 pandemic virus up-regulated inflammatory, apoptotic and T-lymphocyte
167 signaling pathways. Elevated virulence manifested as increased PA expression,
168 ribonucleoprotein polymerase activity and inflammatory response were the effects of
169 PA-X deletion in pH1N1 and highly pathogenic H5N1 avian influenza viruses (Gao et
170 al., 2015). PA-X is also an anti-virulence factor of avian H5N1 virus in avian species
171 as well as in mice (Hu et al., 2015). H5N1 PA-X blunted the global host response in
172 chicken lungs, which included markedly down-regulated genes associated with
173 inflammation and cell death, and promoted anti-apoptotic activity in chicken and duck
174 fibroblasts (Hu et al., 2015). In the present study, we found that PA-X played an
175 opposite role in H9N2 virus. Apoptotic and inflammatory responses were decreased
176 with H9N2 PA-X deficient virus. These observations indicate that the pro- or
177 anti-virulence role of PA-X in influenza viruses is virus strain specific.

178 Loss of PA-X expression decreased viral replication of H9N2 virus *in vivo*. H9N2

PA-X deficient virus showed lower replication levels in mice than H9N2 WT at 3, 5 and 7 dpi. The poor replication in murine lungs was directly related to the lower pathogenicity and reduced expression of inflammatory cytokines from H9N2 PA-X deficient virus infection. Hu J *et al.* (2015) showed that PA-X decreases the virulence of H5N1 virus through inhibiting viral replication and the host innate immune response. Jagger *et al.* (2012) showed that loss of PA-X in 1918 H1N1 virus did not affect viral replication in mice but increased pathogenicity through enhanced host immune response.

Influenza virus infection can induce host shut off with rapid decline of host protein synthesis (Katze *et al.*, 1986a; Katze *et al.*, 1986b) to divert host resources towards viral replication. Inhibition of host protein synthesis also aids in dampening the anti-viral response. Therefore, virus induced host shut off is closely related to viral replication and pathogenicity. Recently, the roles of PA and PA-X in the inhibition of cellular protein synthesis were demonstrated (Desmet et al., 2013; Jagger et al., 2012). The N-terminal domain of PA, which includes the endonuclease active site, is sufficient to suppress protein expression, and PA-X showed a stronger effect than the corresponding N-terminal domain of PA. We previously showed that the absence of PA-X made PA less able to suppress co-transfected gene expression for pH1N1 and H5N1 viruses (Gao et al., 2015). Conceivably, loss of PA-X in these viruses could less effectively inhibit host protein synthesis, which would result in reduced viral replication and virulence. However, loss of PA-X does enhance the virulence of 1918 H1N1, pH1N1 and H5N1 viruses (Gao et al., 2015; Hu et al., 2015; Jagger et al.,

2012). We speculate that the decrease in suppression of host protein synthesis exacerbates host inflammatory response and enhances apoptosis. As 1918 H1N1, pH1N1 and highly pathogenic H5N1 viruses could elicit significantly high levels of pro-inflammatory cytokines, loss of PA-X in such viruses could lead to more severe lung injury and contribute to the enhanced virulence (Kang et al., 2011; Ma et al., 2011; Perrone et al., 2008). In the present study, H9N2 virus is largely a low pathogenicity virus and does not typically induce high levels of cytokines. PA protein in H9N2 virus was less able to suppress GFP expression in the absence of PA-X, suggesting that PA-X also plays a role in the inhibition of host protein synthesis. The level of host shut off by H9N2-FS could be less effective in promoting viral replication but more effective in eliciting an antiviral response. In summary, our results show that PA-X of H9N2 virus, unlike the more virulent H5N1, pH1N1 and 1918 H1N1 viruses, is a pro-virulence factor in the facilitation of viral replication and pathogenicity, and that function of PA-X is virus strain specific. Therefore, the role of PA-X in other influenza viruses needs to be investigated.

Methods

Viruses and cells

A/chicken/Hebei/LC/2008 (HB/08, H9N2) virus was isolated from a diseased chicken in Hebei province, China, in January 2008 and propagated in 10 day-old specific-pathogen-free (SPF) embryonated chicken eggs (Sun et al., 2011). 293T, MDCK, and A549 cells were maintained in Dulbecco's modified Eagle's medium (DMEM; Life Technologies, Foster City, CA, USA) supplemented with 10% fetal

223 bovine serum (FBS; Life Technologies), 100 units/ml of penicillin and 100 g/ml of
224 streptomycin.

225 **Generation of recombinant viruses by reverse genetics**

226 All eight gene segments have been previously amplified by reverse
227 transcription-PCR (RT-PCR) from HB/08 virus and cloned into the dual-promoter
228 plasmid, pHW2000 (Sun et al., 2011). PA-X deficient virus, H9N2-FS, was created by
229 site-directed mutagenesis (QuikChange mutagenesis kit, Agilent) on the
230 corresponding PA gene of H9N2 WT virus, which converted the frameshifting motif
231 from UCC UUU CGU to AGC UUC AGA (U592A, C593G, U597C, C598A and
232 U600A) to prevent the formation of PA-X (Jagger et al., 2012). PCR primer sequences
233 used are available upon request. PA ORF was unaltered in H9N2-FS. Rescued viruses
234 were detected using hemagglutination assays. The viruses were purified by sucrose
235 density gradient centrifugation, and viral RNA was extracted and analyzed by
236 RT-PCR, and each viral segment was sequenced to confirm sequence identity.

237 **Viral titration and replication kinetics**

238 Fifty % tissue culture infective dose ($TCID_{50}$) was determined in MDCK cells
239 using 10-fold serially diluted virus inoculated at 37°C and cultured for 72 h. The
240 $TCID_{50}$ values were calculated by the method of Reed and Muench (Reed & Muench,
241 1938). MDCK and A549 cells were infected with viruses at an MOI of 0.01, overlaid
242 with serum-free DMEM containing 2μg/ml TPCK-trypsin (Sigma–Aldrich) and
243 incubated at 37°C. Supernatants of infected MDCK and A549 cells were harvested at
244 6, 12, 24, 36, 48, 60, 72 and 84 hpi. Virus titers were determined by $TCID_{50}$ in MDCK

cells. Three independent experiments were performed.

Mouse infections

Fifteen mice (six week-old female BALB/c; Vital River Laboratory, Beijing, China) per group were anesthetized with Zoletil (tiletamine-zolazepam; Virbac S.A., Carros, France; 20 μg/g) and inoculated intranasally with 50 μl of 10^6 $TCID_{50}$ of H9N2 diluted in phosphate-buffered saline (PBS). All mice were monitored daily for 14 days, and mice losing 30% of their original body weight were humanely euthanized. Three mice were euthanized on 3, 5 and 7 dpi for the determination of lung virus titers, histopathology and cytokine levels. Lungs were collected and homogenized in cold PBS. Virus titers were determined by $TCID_{50}$. All animal research was approved by the Beijing Association for Science and Technology and complied with Beijing Laboratory Animal Welfare and Ethical Guidelines as issued by the Beijing Administration Committee of Laboratory Animals.

Histopathology

A portion of the lung from each euthanized mouse at 5 dpi was fixed in 10% phosphate-buffered formalin and processed for paraffin embedding. Each 5 μm section was stained with hematoxylin and eosin and examined for histopathological changes. Images were captured with a Zeiss Axioplan 2IE epifluorescence microscope.

Quantification of cytokine/chemokine protein levels in mouse lungs

Levels of cytokines/chemokines including IFN-γ, IL-1β, IL-6, KC, TNF-α, MIP-1α or CCL3 and MCP-1 in lungs were determined by cytometric bead array

assays (BD Cytometric BEAD Array Mouse Inflammation Kit; BD Bioscience, San Diego, CA, USA). Briefly, 50 µl mouse inflammation capture bead suspension and 50 µl detection reagent were added to an equal amount of sample and incubated in the dark for 2 h at room temperature. Subsequently, each sample was washed with 1 ml wash buffer and then centrifuged at 200 × *g* at room temperature for 5 min. Supernatants were discarded and a further 300 µl wash buffer was added. Samples were analyzed on a BD FACS Array bioanalyzer (BD Bioscience). Data were analyzed using BD CBA Software (BD Bioscience). Each chemokine or cytokine was computed as pg/ml of homogenate.

Cell death assays

Virus infection assays were conducted in 6 well plates. Cells were seeded at a density of 1×10^6 cells/well for overnight incubation in infection media (cell growth media with 1% bovine serum albumin was used in place of FBS). Cells were then infected with virus at 1.0 MOI for 12 h. Cells pooled from the supernatant and monolayer were then harvested, washed and stained with FITC labeled annexin V and propidium iodide (PI) (Becton Dickinson, San Jose, CA) for 20 min. After a final wash, cells were resuspended in 100 µl FACs wash buffer (PBS containing 3% BSA and 0.01% sodium azide) and analyzed on the FACs Calibur (BD Biosciences) with Flow Jo software (version 7.6.1). Cell death (apoptosis and necrosis) was defined as annexin-V^+ and PI^+, while apoptotic cells were annexin-V^+ only. Viable cells were considered as neither annexin-V nor PI positive.

Western blotting

289 Total cell protein lysates were extracted from transfected 293T cells or infected
290 MDCK cells with CA630 lysis buffer (150 mM NaCl, 1% CA630 detergent, 50 mM
291 Tris base [pH 8.0]). Cellular proteins were separated by 12% sodium dodecyl
292 sulfate-polyacrylamide gel electrophoresis (SDS-PAGE) and transferred to a
293 polyvinylidene difluoride (PVDF) membrane (Amersham Biosciences, Germany).
294 Each PVDF membrane was blocked with 0.1% Tween 20 and 5% nonfat dry milk in
295 Tris-buffered saline and subsequently incubated with a primary antibody. Primary
296 antibodies were specific for influenza A virus PA (1:3000, GeneTex, USA), influenza
297 A virus PA-X [diluted 1:2000, polyclonal rabbit antiserum against a H5N1 X-ORF
298 derived peptide(CAGLPTKVSHRTSPA), Genscript, China)], influenza A virus PB1
299 (diluted 1:3000, Thermo Fisher Scientific, USA), GFP (1:1000, Abcam, UK), β-actin
300 (1:1000, Santa Cruz, USA). The secondary antibody used was either horseradish
301 peroxidase (HRP)-conjugated anti-mouse antibody or HRP-conjugated anti-rabbit
302 antibody (diluted 1:10,000 Jackson ImmunoResearch USA), as appropriate. HRP
303 presence was detected using a Western Lightning chemiluminescence kit (Amersham
304 Pharmacia, Freiburg, Germany), following the manufacturer's protocol.

305 **Statistics**

306 All statistical analyses were performed using GraphPad Prism Software Version
307 5.0 (GraphPad Software Inc., San Diego, CA, USA). The two treatment methods were
308 compared by two-tailed Student's t-test, and multiple comparisons were carried out by
309 two-way analysis of variance (ANOVA) considering time and virus as factors.
310 Differences were considered statistically significant at $P < 0.05$. All data are reported

311 as the mean ± standard deviation (SD).

312

313 **Acknowledgments**

314 This work was supported by the National Natural Science Foundation of China (No.

315 31302102 and No. 31430086), the National Basic Research Program (973 Program)

316 (No. 2011CB504702), and a grant from the Chang Jiang Scholars Program.

317

References

Abolnik, C., Gerdes, G. H., Sinclair, M., Ganzevoort, B. W., Kitching, J. P., Burger, C. E., Romito, M., Dreyer, M., Swanepoel, S., Cumming, G. S. & Olivier, A. J. (2010). Phylogenetic analysis of influenza A viruses (H6N8, H1N8, H4N2, H9N2, H10N7) isolated from wild birds, ducks, and ostriches in South Africa from 2007 to 2009. *Avian Dis* **54**, 313-322.

Banks, J., Speidel, E. C., Harris, P. A. & Alexander, D. J. (2000). Phylogenetic analysis of influenza A viruses of H9 haemagglutinin subtype. *Avian Pathol* **29**, 353-359.

Bano, S., Naeem, K. & Malik, S. A. (2003). Evaluation of pathogenic potential of avian influenza virus serotype H9N2 in chickens. *Avian Dis* **47**, 817-822.

Bermejo-Martin, J. F., Martin-Loeches, I., Rello, J., Antón, A., Almansa, R., Xu, L., Lopez-Campos, G., Pumarola, T., Ran, L. & Ramirez, P. (2010). Host adaptive immunity deficiency in severe pandemic influenza. *Crit Care* **14**, R167.

Butt, A. M., Siddique, S., Idrees, M. & Tong, Y. (2010). Avian influenza A (H9N2): computational molecular analysis and phylogenetic characterization of viral surface proteins isolated between 1997 and 2009 from the human population. *Virol J* **7**, 319.

Butt, K. M., Smith, G. J., Chen, H., Zhang, L. J., Leung, Y. H., Xu, K. M., Lim, W., Webster, R. G., Yuen, K. Y., Peiris, J. S. & Guan, Y. (2005). Human infection with an avian H9N2 influenza A virus in Hong Kong in 2003. *J Clin*

Microbiol **43**, 5760-5767.

Capua, I. & Alexander, D. J. (2006). The challenge of avian influenza to the veterinary community. *Avian Pathol* **35**, 189-205.

Chanturiya, A. N., Basanez, G., Schubert, U., Henklein, P., Yewdell, J. W. & Zimmerberg, J. (2004). PB1-F2, an influenza A virus-encoded proapoptotic mitochondrial protein, creates variably sized pores in planar lipid membranes. *J Virol* **78**, 6304-6312.

Chen, H., Yuan, H., Gao, R., Zhang, J., Wang, D., Xiong, Y., Fan, G., Yang, F., Li, X., Zhou, J., Zou, S., Yang, L., Chen, T., Dong, L., Bo, H., Zhao, X., Zhang, Y., Lan, Y., Bai, T., Dong, J., Li, Q., Wang, S., Li, H., Gong, T., Shi, Y., Ni, X., Li, J., Fan, J., Wu, J., Zhou, X., Hu, M., Wan, J., Yang, W., Li, D., Wu, G., Feng, Z., Gao, G. F., Wang, Y., Jin, Q., Liu, M. & Shu, Y. (2014). Clinical and epidemiological characteristics of a fatal case of avian influenza A H10N8 virus infection: a descriptive study. *Lancet* **383**, 714-721.

Chen, W., Calvo, P. A., Malide, D., Gibbs, J., Schubert, U., Bacik, I., Basta, S., O'Neill, R., Schickli, J., Palese, P., Henklein, P., Bennink, J. R. & Yewdell, J. W. (2001). A novel influenza A virus mitochondrial protein that induces cell death. *Nat Med* **7**, 1306-1312.

Coman, A., Maftei, D. N., Krueger, W. S., Heil, G. L., Friary, J. A., Chereches, R. M., Sirlincan, E., Bria, P., Dragnea, C., Kasler, I. & Gray, G. C. (2013). Serological evidence for avian H9N2 influenza virus infections among Romanian agriculture workers. *J Infect Public Health* **6**, 438-447.

Cong, Y. L., Pu, J., Liu, Q. F., Wang, S., Zhang, G. Z., Zhang, X. L., Fan, W. X., Brown, E. G. & Liu, J. H. (2007). Antigenic and genetic characterization of H9N2 swine influenza viruses in China. *J Gen Virol* **88**, 2035-2041.

Desmet, E. A., Bussey, K. A., Stone, R. & Takimoto, T. (2013). Identification of the N-Terminal Domain of the Influenza Virus PA Responsible for the Suppression of Host Protein Synthesis. *J Virol* **87**, 3108-3118.

Gao, H., Sun, Y., Hu, J., Qi, L., Wang, J., Xiong, X., Wang, Y., He, Q., Lin, Y., Kong, W., Seng, L. G., Sun, H., Pu, J., Chang, K. C., Liu, X. & Liu, J. (2015). The contribution of PA-X to the virulence of pandemic 2009 H1N1 and highly pathogenic H5N1 avian influenza viruses. *Sci Rep* **5**, 8262.

Gao, R., Cao, B., Hu, Y., Feng, Z., Wang, D., Hu, W., Chen, J., Jie, Z., Qiu, H., Xu, K., Xu, X., Lu, H., Zhu, W., Gao, Z., Xiang, N., Shen, Y., He, Z., Gu, Y., Zhang, Z., Yang, Y., Zhao, X., Zhou, L., Li, X., Zou, S., Zhang, Y., Yang, L., Guo, J., Dong, J., Li, Q., Dong, L., Zhu, Y., Bai, T., Wang, S., Hao, P., Yang, W., Han, J., Yu, H., Li, D., Gao, G. F., Wu, G., Wang, Y., Yuan, Z. & Shu, Y. (2013). Human infection with a novel avian-origin influenza A (H7N9) virus. *N Engl J Med* **368**, 1888-1897.

Hagau, N., Slavcovici, A., Gonganau, D. N., Oltean, S., Dirzu, D. S., Brezoszki, E. S., Maxim, M., Ciuce, C., Mlesnite, M. & Gavrus, R. L. (2010). Clinical aspects and cytokine response in severe H1N1 influenza A virus infection. *Crit Care* **14**, R203.

Hu, J., Mo, Y., Wang, X., Gu, M., Hu, Z., Zhong, L., Wu, Q., Hao, X., Hu, S., Liu,

W., Liu, H. & Liu, X. (2015). PA-X Decreases the Pathogenicity of Highly Pathogenic H5N1 Influenza A Virus in Avian Species by Inhibiting Virus replication and Host Response. *J Virol* **89**, 4126-4142.

Jagger, B., Wise, H., Kash, J., Walters, K.-A., Wills, N., Xiao, Y.-L., Dunfee, R., Schwartzman, L., Ozinsky, A. & Bell, G. (2012). An overlapping protein-coding region in influenza A virus segment 3 modulates the host response. *Science* **337**, 199-204.

Jia, N., de Vlas, S. J., Liu, Y. X., Zhang, J. S., Zhan, L., Dang, R. L., Ma, Y. H., Wang, X. J., Liu, T., Yang, G. P., Wen, Q. L., Richardus, J. H., Lu, S. & Cao, W. C. (2009). Serological reports of human infections of H7 and H9 avian influenza viruses in northern China. *J Clin Virol* **44**, 225-229.

Kang, Y. M., Song, B. M., Lee, J. S., Kim, H. S. & Seo, S. H. (2011). Pandemic H1N1 influenza virus causes a stronger inflammatory response than seasonal H1N1 influenza virus in ferrets. *Arch Virol* **156**, 759-767.

Katze, M. G., DeCorato, D. & Krug, R. M. (1986a). Cellular mRNA translation is blocked at both initiation and elongation after infection by influenza virus or adenovirus. *J Virol* **60**, 1027-1039.

Katze, M. G., Detjen, B. M., Safer, B. & Krug, R. M. (1986b). Translational control by influenza virus: suppression of the kinase that phosphorylates the alpha subunit of initiation factor eIF-2 and selective translation of influenza viral mRNAs. *Mol Cell Biol* **6**, 1741-1750.

Lam, W. Y., Yeung, A., Chu, I. & Chan, P. (2010). Profiles of cytokine and

406 chemokine gene expression in human pulmonary epithelial cells induced by
407 human and avian influenza viruses. *Virol J* **7**, 344.
408 **Lin, Y. P., Shaw, M., Gregory, V., Cameron, K., Lim, W., Klimov, A., Subbarao,**
409 **K., Guan, Y., Krauss, S., Shortridge, K., Webster, R., Cox, N. & Hay, A.**
410 **(2000).** Avian-to-human transmission of H9N2 subtype influenza A viruses:
411 relationship between H9N2 and H5N1 human isolates. *Proc Natl Acad Sci U S*
412 *A* **97**, 9654-9658.
413 **Ma, W., Belisle, S. E., Mosier, D., Li, X., Stigger-Rosser, E., Liu, Q., Qiao, C.,**
414 **Elder, J., Webby, R. & Katze, M. G. (2011).** 2009 pandemic H1N1 influenza
415 virus causes disease and upregulation of genes related to inflammatory and
416 immune responses, cell death, and lipid metabolism in pigs. *J Virol* **85**,
417 11626-11637.
418 **Perrone, L. A., Plowden, J. K., García-Sastre, A., Katz, J. M. & Tumpey, T. M.**
419 **(2008).** H5N1 and 1918 pandemic influenza virus infection results in early and
420 excessive infiltration of macrophages and neutrophils in the lungs of mice.
421 *PLoS pathog* **4**, e1000115.
422 **Reed, L. J. & Muench, H. (1938).** A simple method of estimating fifty per cent
423 endpoints. *Am J Epidemiol* **27**, 493-497.
424 **Roberts, N. J., Jr. & Nichols, J. E. (1989).** Regulation of lymphocyte proliferation
425 after influenza virus infection of human mononuclear leukocytes. *J Med Virol*
426 **27**, 179-187.
427 **Sun, Y., Pu, J., Jiang, Z., Guan, T., Xia, Y., Xu, Q., Liu, L., Ma, B., Tian, F.,**

Brown, E. G. & Liu, J. (2010). Genotypic evolution and antigenic drift of H9N2 influenza viruses in China from 1994 to 2008. *Vet Microbiol* **146**, 215-225.

Sun, Y., Qin, K., Wang, J., Pu, J., Tang, Q., Hu, Y., Bi, Y., Zhao, X., Yang, H. & Shu, Y. (2011). High genetic compatibility and increased pathogenicity of reassortants derived from avian H9N2 and pandemic H1N1/2009 influenza viruses. *Proc Natl Acad Sci USA* **108**, 4164-4169.

Tumpey, T. M., Lu, X., Morken, T., Zaki, S. R. & Katz, J. M. (2000). Depletion of lymphocytes and diminished cytokine production in mice infected with a highly virulent influenza A (H5N1) virus isolated from humans. *J Virol* **74**, 6105-6116.

Wang, M., Fu, C. X. & Zheng, B. J. (2009). Antibodies against H5 and H9 avian influenza among poultry workers in China. *N Engl J Med* **360**, 2583-2584.

Xu, K. M., Smith, G. J., Bahl, J., Duan, L., Tai, H., Vijaykrishna, D., Wang, J., Zhang, J. X., Li, K. S., Fan, X. H., Webster, R. G., Chen, H., Peiris, J. S. & Guan, Y. (2007). The genesis and evolution of H9N2 influenza viruses in poultry from southern China, 2000 to 2005. *J Virol* **81**, 10389-10401.

Zhang, Q., Shi, J., Deng, G., Guo, J., Zeng, X., He, X., Kong, H., Gu, C., Li, X., Liu, J., Wang, G., Chen, Y., Liu, L., Liang, L., Li, Y., Fan, J., Wang, J., Li, W., Guan, L., Li, Q., Yang, H., Chen, P., Jiang, L., Guan, Y., Xin, X., Jiang, Y., Tian, G., Wang, X., Qiao, C., Li, C., Bu, Z. & Chen, H. (2013). H7N9 influenza viruses are transmissible in ferrets by respiratory droplet. *Science*

341, 410-414.

Zhirnov, O. P., Konakova, T. E., Wolff, T. & Klenk, H. D. (2002). NS1 protein of influenza A virus down-regulates apoptosis. *J Virol* **76**, 1617-1625.

Figure legends

Figure 1. Generation of H9N2 PA-X deficient viruses. (a) The frameshifting motif of UCC UUU CGU was mutated to AGC UUC AGA (in red) in the PA gene which did not alter the PA ORF but abrogated the expression of PA-X. (b) PA-X protein expression was abolished in H9N2-FS virus infected cells. MDCK cells were infected with H9N2-FS and H9N2 WT virus for 12 h. Western blotting was performed on cell lysates with antibodies against PA-X or PB1 or β-actin, as indicated, followed by AP-conjugated secondary antibodies.

Figure 2. Growth of H9N2 WT and FS viruses and induction of apoptosis. Virus growth curves of H9N2 WT and H9N2-FS viruses in MDCK cells (a) and A549 (b) cells over 84 h. (c) Cell death was determined in A549 cells by detection of annexin$^+$ and/or PI$^+$ at 6 and 12 hpi of H9N2 WT or H9N2-FS virus at 1.0 MOI. Representative dual-labeled quadrants of bivariant fluorescence dot plots showing the induction of apoptosis in infected cells. Apoptotic cells, positive for annexin V but not PI, were identified in the right lower quadrant. Cells positive for PI but not annexin V (indicative of necrosis) were identified in the right upper quadrant. MOCK = uninfected control cells. Each value represents the mean of three independent experiments performed in triplicates; error bars indicate standard deviations (SD). * indicates significant difference between FS virus and wild type virus ($P < 0.05$). .

Figure 3. Pathogenicity of H9N2 WT and H9N2-FS viruses in mice. (a) Reduced survival (percentage) was found with H9N2 WT virus infected mice over a 14 day period (inoculation at day 0). (b) H9N2 WT virus infected mice showed significant

478 weight loss, unlike H9N2-FS virus and mock infected mice. Any mouse that lost more
479 than 30% of its body weight was euthanized. (c) Histopathology in lung of H9N2-FS
480 virus infected mice was mild to normal compared with corresponding H9N2 WT virus
481 infection which showed vascular congestion and cellular infiltration of bronchioles
482 and alveoli. Scale bars, 100 μm. (d) Mean of viral lung load ± SD was based on $\log_{10}$
483 $TCID_{50}$ determination in MDCK cells. * indicates significant difference between
484 H9N2 WT and H9N2-FS virus ($P < 0.05$). Means of the data of three mice per group
485 are shown, and error bars are SDs.

486 **Figure 4. Detection of cytokine/chemokine proteins in lungs of mice infected with**
487 **H9N2 WT and H9N2-FS viruses.** Mean cytokine/chemokine levels ± SDs are shown
488 (n=3). * indicates significant difference between H9N2-FS and H9N2 WT ($P < 0.05$).

489 **Figure 5. PA without PA-X is less able to suppress co-expressed GFP in 293T cells.**
490 (a) eGFP expression plasmid was co-transfected with PA plasmid derived from H9N2
491 WT or H9N2-FS viruses, or with mock plasmid (control pcDNA3.1). eGFP
492 fluorescence was captured at 24 h post transfection. GFP fluorescence (green) is
493 shown in the left panel, and merged with DAPI staining fluorescence is shown in the
494 right panel. The GFP expression levels were quantified by fluorescence intensity. The
495 fluorescence intensities were analyzed with Image-Pro-Plus (Media Cybernetics).
496 Relative fluorescence intensity of each group as compared with control was shown as
497 histograms. Values shown are means of the results of three independent experiments ±
498 SDs. (b) PA and GFP protein expression were determined by Western blotting analysis
499 using anti-PA and anti-GFP antibody. Anti-β-actin antibody was used as loading

control. Protein bands were quantified by densitometry. Protein levels of PA and GFP relative to β-actin are shown as histograms. Stronger expression of PA, in the absence of PA-X, derived from H9N2-FS virus did not lead greater inhibition of GFP expression. The results shown are representative data from three independent experiments. Error bars indicate SDs. * indicates significant difference between H9N2 WT and H9N2-FS virus ($P < 0.05$).

(a)

		592		600
Nucleotide Sequence Of PA	WT	UCC	UUU	CGU
	FS	AGC	UUC	AGA
Amino Acids Of PA		190 S	191 F	192 R

(b)

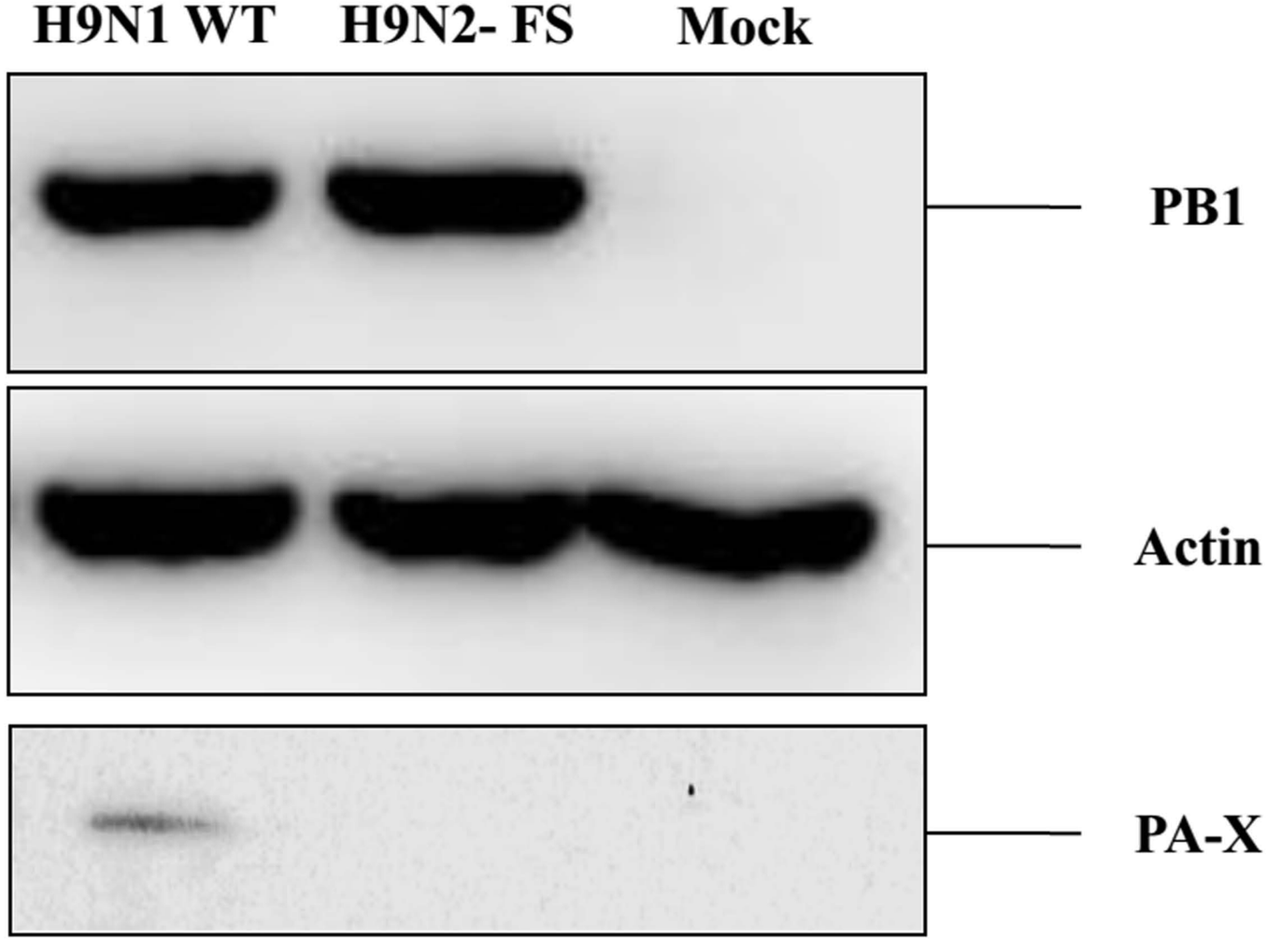

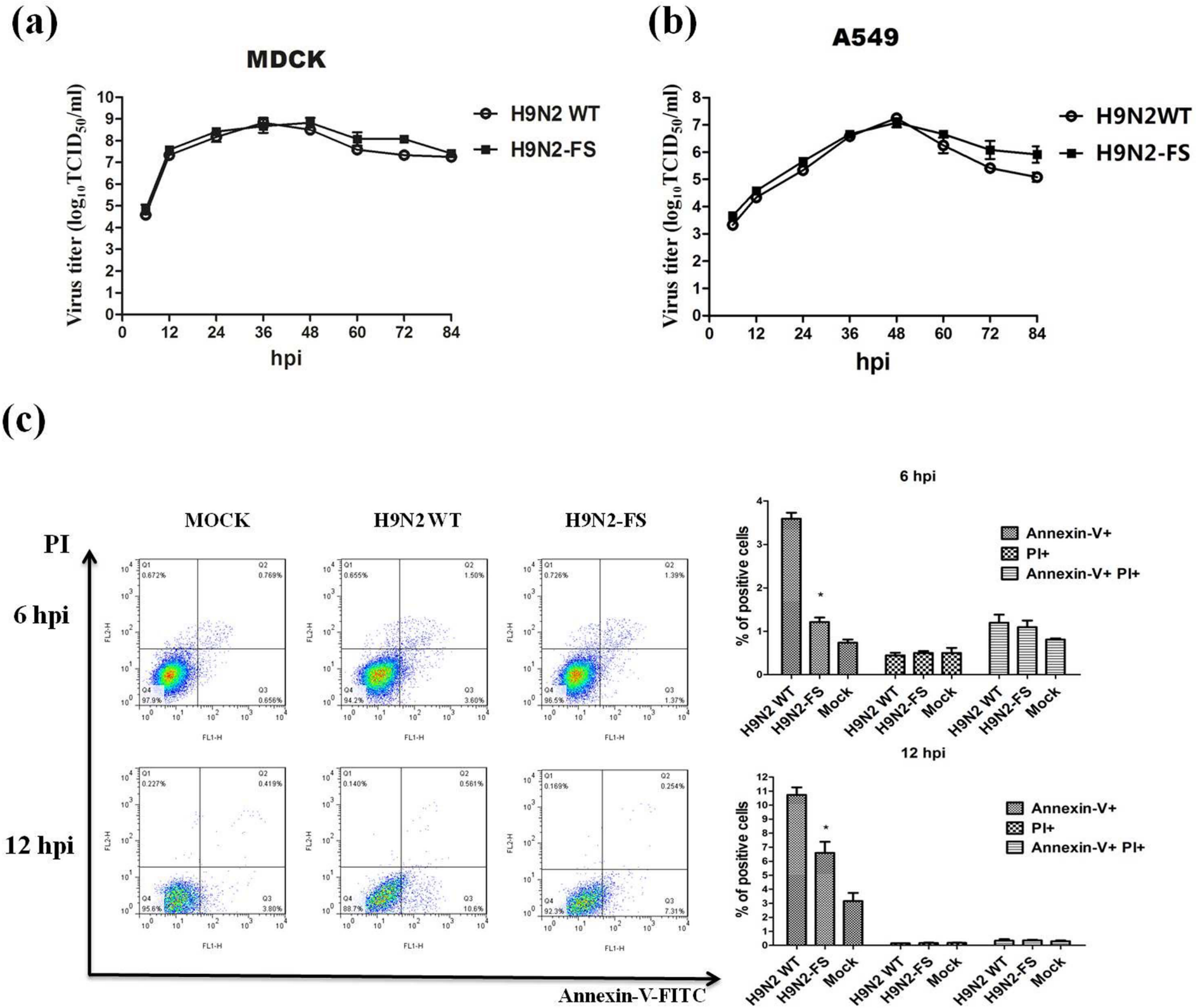
(a)
MDCK
Virus titer (log_{10}TCID$_{50}$/ml)
hpi
H9N2 WT
H9N2-FS
(b)
A549
Virus titer (log_{10}TCID$_{50}$/ml)
hpi
H9N2WT
H9N2-FS
(c)
MOCK
H9N2 WT
H9N2-FS
PI
6 hpi
12 hpi
Annexin-V-FITC
6 hpi
% of positive cells
Annexin-V+
PI+
Annexin-V+ PI+
H9N2 WT
H9N2-FS
Mock
12 hpi

(a)

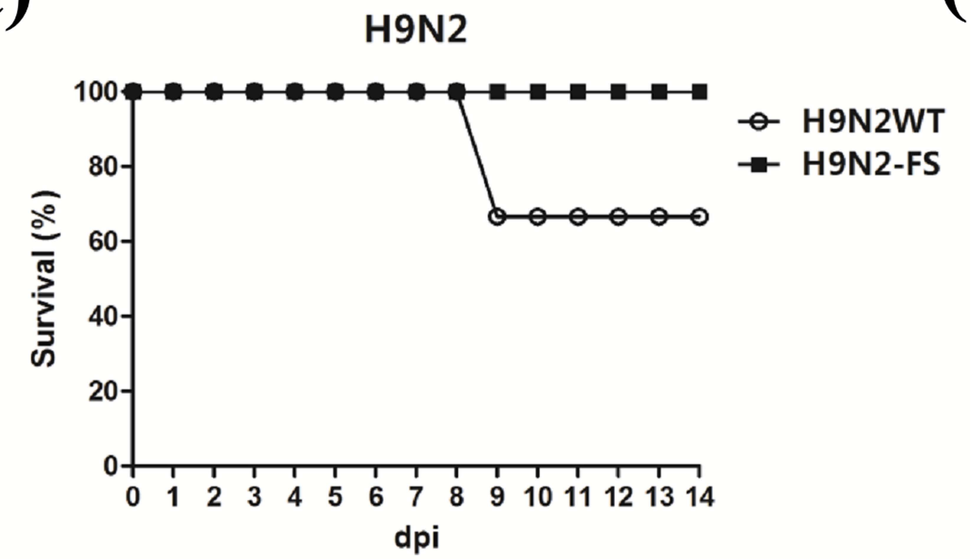
H9N2
Survival (%)
dpi
H9N2WT
H9N2-FS

(b)

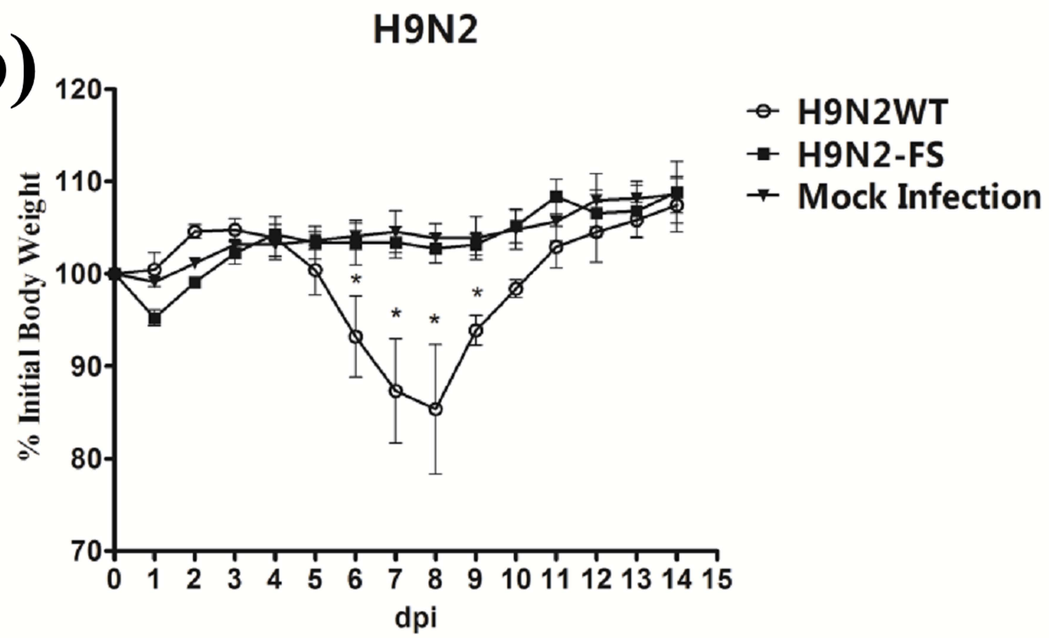
H9N2
% Initial Body Weight
dpi
H9N2WT
H9N2-FS
Mock Infection

(c)

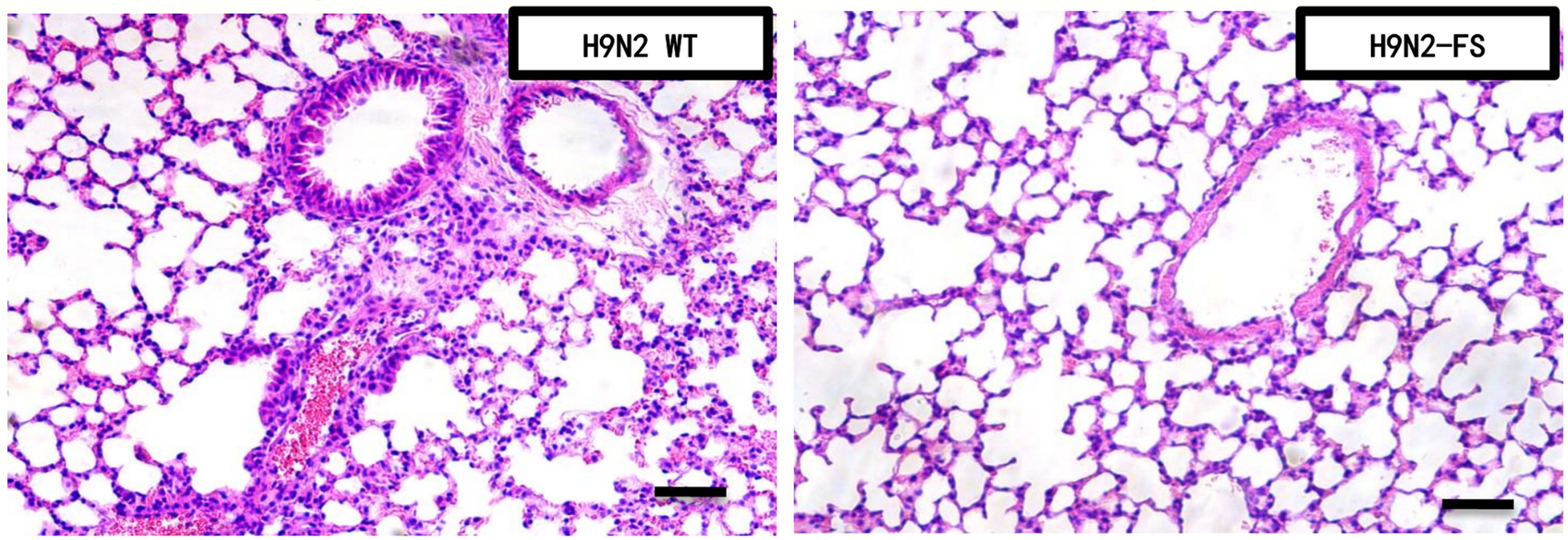
H9N2 WT
H9N2-FS

(d)

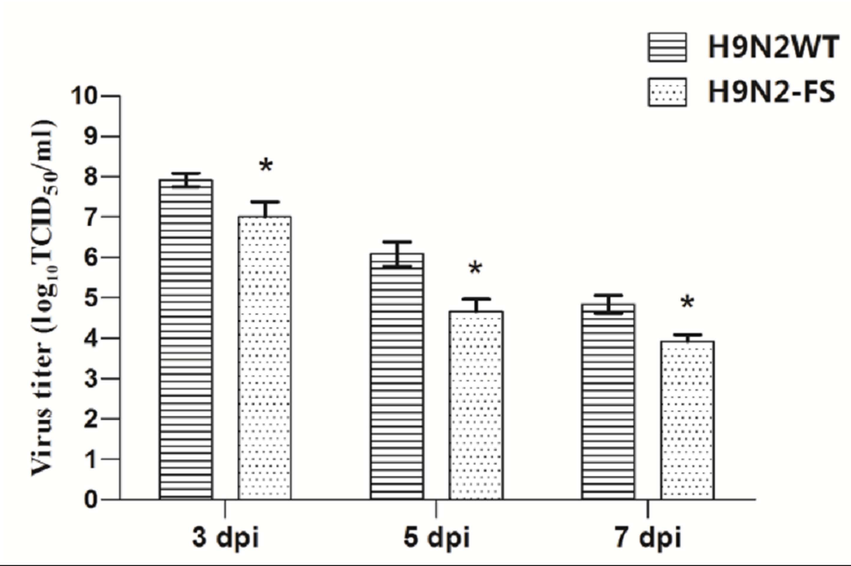
H9N2WT
H9N2-FS
Virus titer (log10TCID50/ml)
3 dpi
5 dpi
7 dpi

H9N2WT
H9N2-FS
Mock Infection

IFN-γ

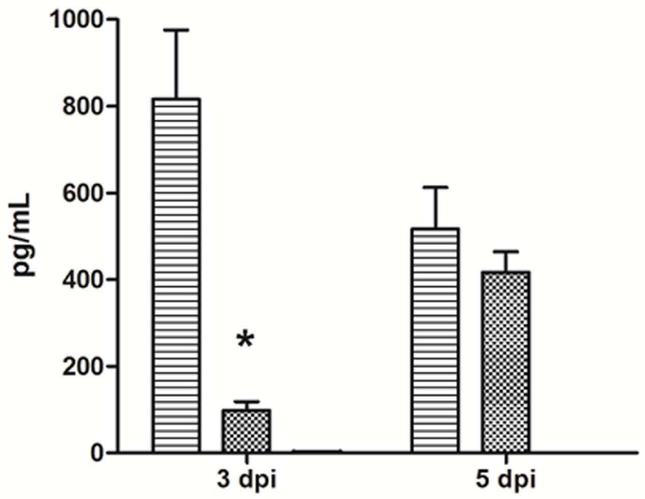

IL-1β

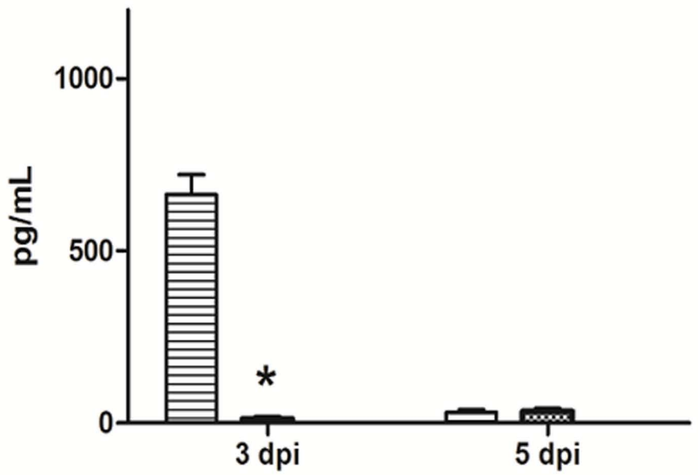

IL-6

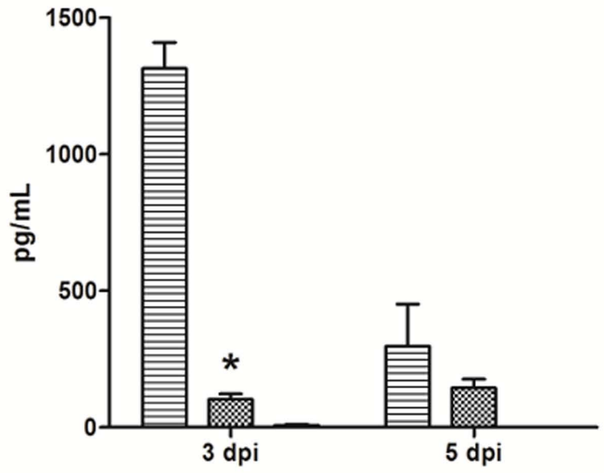

KC

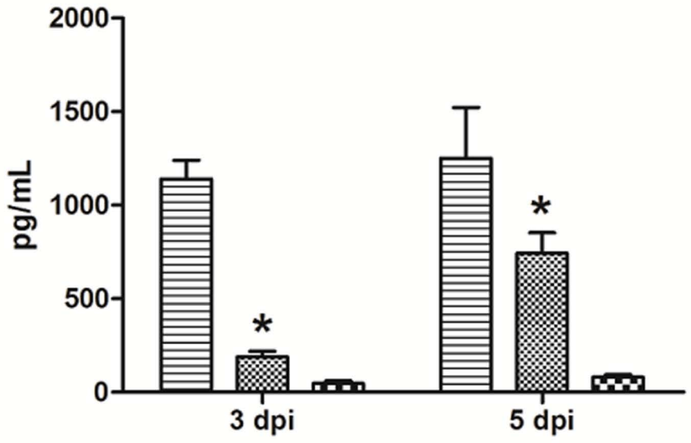

TNF-α

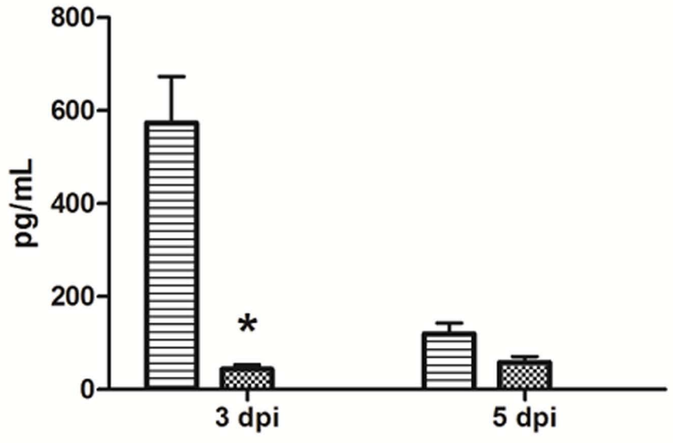

MIP-1α

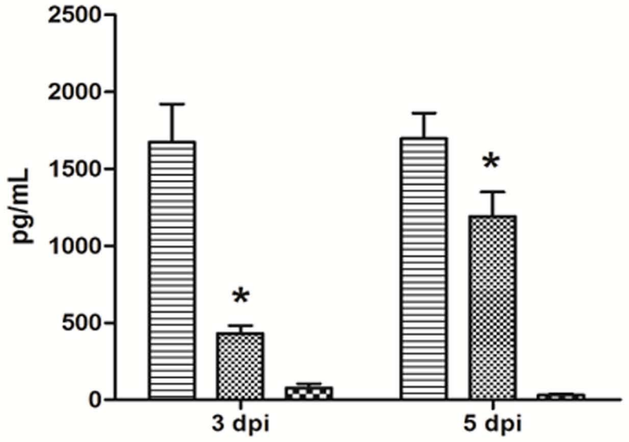

MCP-1

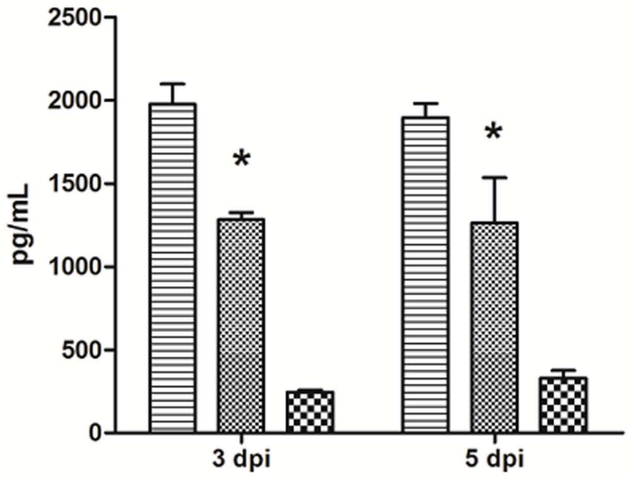

(a)

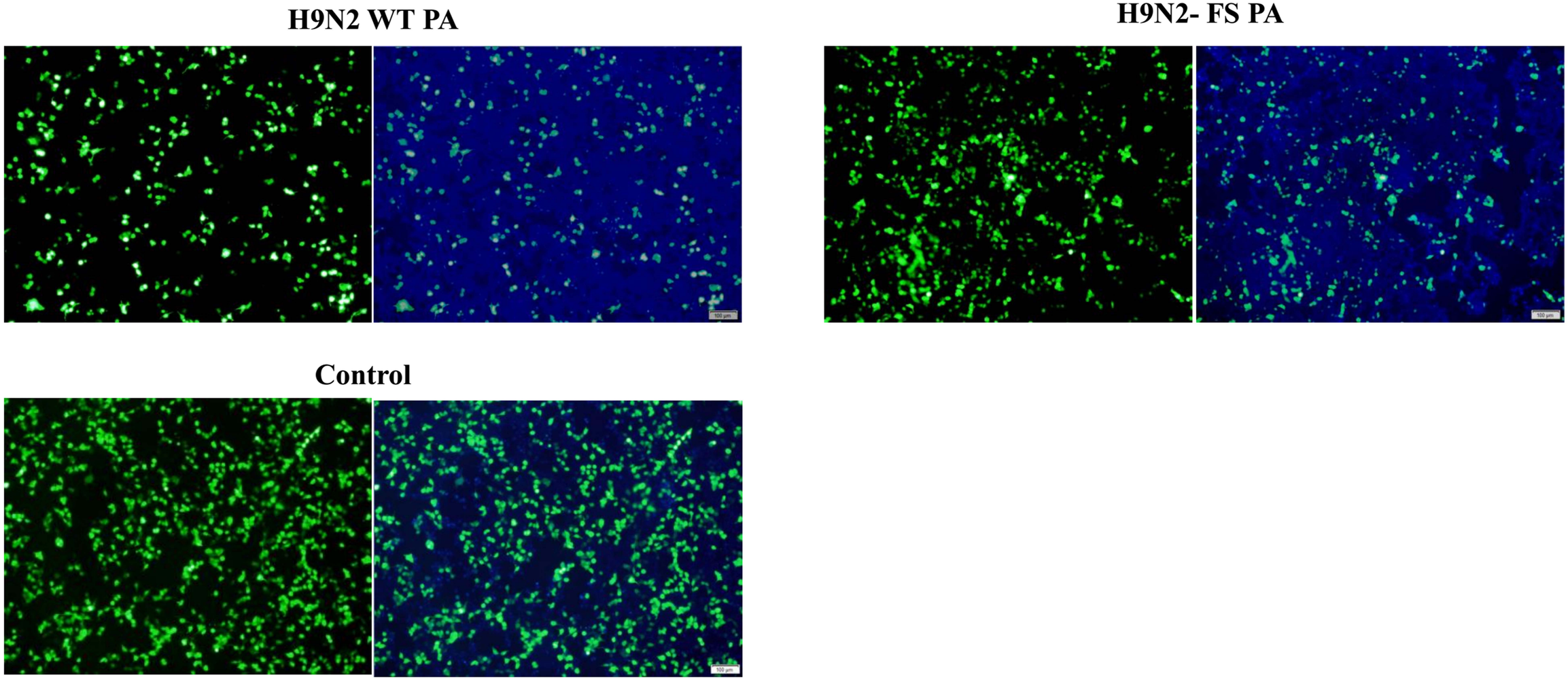
H9N2 WT PA
H9N2- FS PA
Control

(b)

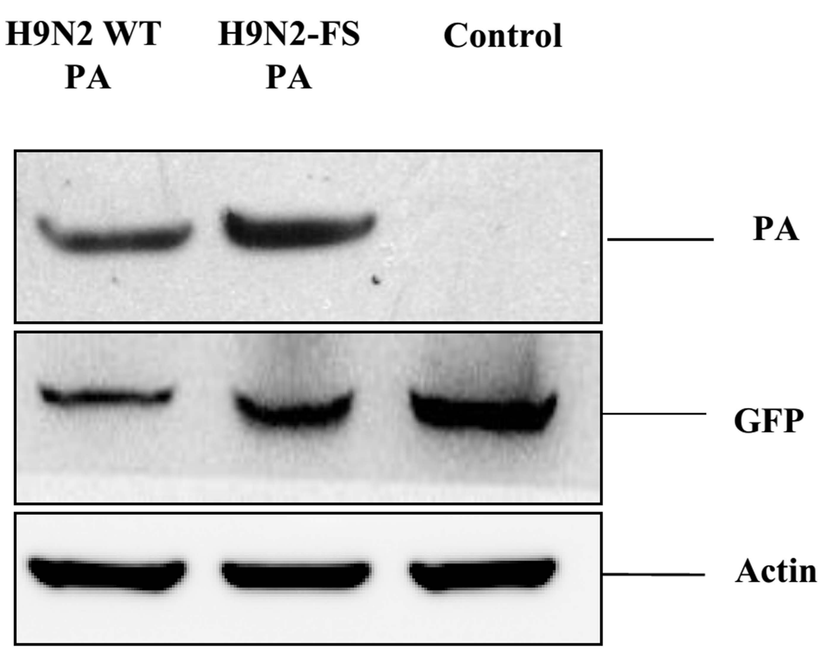
H9N2 WT PA
H9N2-FS PA
Control
PA
GFP
Actin

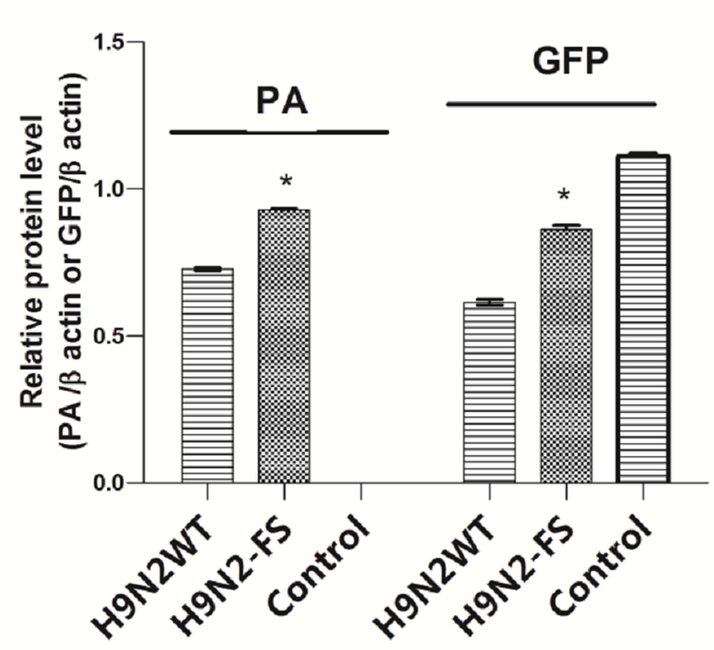
PA
GFP
Relative protein level (PA /β actin or GFP/β actin)
1.5
1.0
0.5
0.0
*
*
H9N2WT
H9N2-FS
Control
H9N2WT
H9N2-FS
Control